Numerical Investigation of Energy Desorption in Dual Metal Hydride Bed based Thermochemical Energy Storage System

Sumeet Kumar Dubey[1], K. Ravi Kumar[1], Vinay Tiwari[2] and Umish Srivastva[2]

[1] Indian Institute of Technology (IIT) Delhi, New Delhi (India)

[2] Indian Oil Corporation R&D Centre, Faridabad, Haryana (India)

Abstract

Among thermal energy storage (TES) systems, thermochemical energy storage (TCES) systems are known for high energy storage density. Metal hydride (MH) based TCES system, due to its good chemical reversibility and higher thermal stability, found suitable for high temperature TES applications. Many studies have reported the improvement in energy storage characteristics with enhancement in the heat transfer phenomenon in dual MH bed systems. The study investigates the discharging characteristics of a dual MH bed system for high temperature thermal energy release process. The dual metal hydride bed system includes a high temperature metal hydride (HTMH) bed, which works as energy storage media operating at high temperatures and a low-temperature metal hydride (LTMH) bed, used as hydrogen storage media. $NaMgH_2F$ is used as HTMH, while Mg_2NiH_4 is used as LTMH. The heat transfer phenomenon, energy discharging characteristics, and hydrogen transfer during thermal energy release from HTMH are studied. The energy desorbed from the MH bed for thermal conductivity 0.5 W/m K, 0.75 W/m K, and 1 W/m K are found as 251.25 kJ, 258.22 kJ, and 260.57 kJ, respectively. Hydrogen absorbed in the HTMH during thermal energy desorption for thermal conductivity 0.5 W/m K, 0.75 W/m K, and 1 W/m K are 6.94 g, 7.13 g, and 7.17 g, respectively. The heat transfer phenomenon in HTMH bed has improved with the increase in thermal conductivity of HTMH, and hence, the heat desorption characteristics also improved. The thermal energy discharging rate from HTMH also increased with the increase in the thermal conductivity of the HTMH bed.

Keywords: Concentrating solar power, Thermochemical energy storage, High temperature thermal energy storage, Dual metal hydride system.

Introduction

Solar energy has a huge potential to fulfill the thermal energy requirement in industrial process heating and solar thermal power generation. However, the utilization of solar energy has challenges, such as its intermittent nature and diurnal variation hindering the usage of solar energy. A thermal energy storage system (TES) can address the abovementioned issues and utilize solar energy effectively. TES systems can be classified as sensible, latent, and thermochemical energy storage systems (Jain et al., 2021). Sensible energy storage system stores/releases heat by changing the temperature of the working media, while the latent energy storage system stores/releases heat by changing the phase of the storage media. Thermochemical storage system stores/releases heat as an endothermic/exothermic chemical reaction, as shown in the chemical reaction below in Equations 1 and 2. With the limitation of low energy storage density of sensible and latent storage, thermochemical energy storage has recently gained attention. TCES systems are also found thermally stable at high temperatures with good cyclic stability. Metal hydride-based thermochemical systems have better reversibility and long cyclic life as compared to other thermochemical energy systems.

$$MH + \Delta H \rightarrow Metal\,(alloy) + Hydrogen \tag{1}$$

$$NaMgH_2F + \Delta H \rightarrow NaF + Mg + H_2 \qquad (\Delta H = 96.8\ kJ/mol\ H_2) \tag{2}$$

In earlier studies on metal hydrides for thermal energy storage, Magnesium (Mg) and its alloys have been extensively studied because of their higher storage capacity, thermal stability, cyclic stability, and lesser cost. Mg-based metal hydrides have been studied to store waste heat for steam generation application. The system stored 9.08 kWh of heat energy at 370 ºC with storage efficiency near 80% (Bogdanović et al., 1995). A Mg hydride system was also studied for cyclic stability at 420 ºC. 19 gm Mg hydride system was operated for 20 cycles without any change in storage density. The heat losses from the system were significant, but the authors expected a reduction in heat loss with an increase in the size of the system (Paskevicius et al., 2015). Numerical analyses of single bed (Mg_2Ni alloy) HTMH have been performed to study heat transfer, energy absorption,

10.18086/swc.2023.03.06 Available at http://proceedings.ises.org

and desorption (sorption) characteristics (Dubey and Kumar, 2022a, 2022b, 2021a, 2021b). Tubular and annular configurations of Mg_2Ni alloy were compared for charging/discharging time and storage density. The desorption of hydrogen from the annular reactor was found to be 70% fast without much variation in energy storage density (Sunku Prasad and Muthukumar, 2023).

Dual metal hydride-based thermal energy storage systems were also investigated for the system's feasibility and performance. $NaMgH_2F$ and $TiCr_{1.6}Mn_{0.2}$ were used as HTMH and LTMH, respectively and an energy storage density of 226 kWh/m^3 was reported (D'Entremont. et al., 2017). Another dual metal hydride system, which used Mg_2FeH_6 as HTMH and Na_3AlH_6 as LTMH, was investigated. The system was found suitable for the temperature range of 450-500 ºC and energy storage density of 132 kWh/m^3 (D'Entremont et al., 2018). The same pair of metal hydrides used fins as extended surfaces and reported an energy storage density of 90 kWh/m^3 and 96% storage efficiency (Sofiene Mellouli et al., 2018). Another study that used Mg_2Ni alloy as HTMH and $LaNi_5$ alloy as LTMH reported 156 kWh/m^3 energy storage density with an energy storage density of 89.4% (Malleswararao et al., 2020).

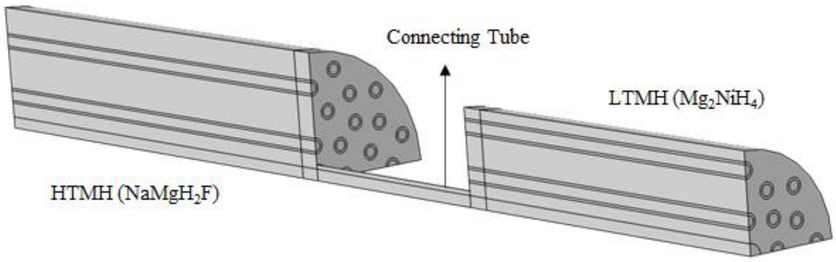

Figure 1: Geometry of coupled metal hydride bed system

This study considers the discharging process of heat at high temperature from a dual metal hydride bed system for performance analysis. $NaMgH_2F$ is used as HTMH, while Mg_2NiH_4 is used as LTMH. One kg of HTMH storage media is considered in a cylindrical shape bed. The HTMH and LTMH beds are embedded with radially distributed axial heat transfer fluid (HTF) tubes and a hydrogen tube at the center coupled by a connecting tube, as shown in Figure 1. Since the HTMH and LTMH are symmetric with respect to the x and y axis, one-fourth of the complete geometry is considered for analysis to minimize the computational time. The LTMH requirement is calculated by considering the quantity of hydrogen released from HTMH.

Mathematical Modelling

This section includes a discussion on the model development in COMSOL Multiphysics. The governing equations, thermochemical properties, assumptions, geometry details, initial values, and boundary conditions used in the model are discussed in detail.

Governing Equation

The mass, momentum, and energy conservation equation used in the numerical analysis are discussed (Dubey and Kumar, 2022b, 2021a; Malleswararao et al., 2020). Equation (3) represents the mass balance equation for hydrogen flowing inside the pores of metal hydride while eq. (4) represents the mass balance equation for the metal hydride fraction. Equation (6) and Equation (7) represent mass balance for HTF (compressed air) and hydrogen flow in tubes.

$$\varepsilon \frac{\partial \rho_g}{\partial t} + \nabla.\left(\rho_g u_g\right) = -S_m \quad (3)$$

$$(1-\varepsilon)\frac{\partial \rho_s}{\partial t} = S_m \quad (4)$$

$$S_m = C_d exp\left(\frac{-E_d}{RT}\right) ln\left(\frac{p}{p_{eq}}\right)(\rho_{sat} - \rho) \quad (5)$$

$$\frac{\partial \rho_g}{\partial t} + \nabla.\left(\rho_g u_g\right) = 0 \quad (6)$$

$$\frac{\partial \rho_a}{\partial t} + \nabla.(\rho_a u_a) = 0 \quad (7)$$

The Brinkman equation represented by equation (8) is used for the momentum balance of hydrogen flow in metal hydride pores. Navier Stokes equation represented by equations (9) and (10) are used for the momentum balance of hydrogen and HTF.

$$\frac{\rho_g}{\varepsilon}\left(\frac{\partial u_g}{\partial t} + u_g.\frac{\nabla u_g}{\varepsilon}\right) = -\nabla p - \frac{\mu_g}{K}u_g - \frac{S_m}{\varepsilon^2}u_g + \nabla.\left[\frac{\mu_g}{\varepsilon}\left(\nabla u_g + \left(\nabla u_g\right)^T\right) - \frac{2\mu_g}{3\varepsilon}(\nabla.u_g)\right] \quad (8)$$

$$\left(\frac{\partial u_g}{\partial t} + u_g.\frac{\nabla u_g}{\varepsilon}\right) = -\nabla p + \nabla.\left[\mu_g\left(\nabla u_g + \left(\nabla u_g\right)^T\right) - \frac{2\mu_g}{3}(\nabla.u_g)\right] \quad (9)$$

$$\left(\frac{\partial u_a}{\partial t} + u_a.\frac{\nabla u_a}{\varepsilon}\right) = -\nabla p + \nabla.\left[\mu_a(\nabla u_a + (\nabla u_a)^T) - \frac{2\mu_a}{3}(\nabla.u_a)\right] \quad (10)$$

Energy balance equations for metal hydride , hydrogen and HTF are represented by equation (10), (15), and (16) respectively. Effective thermal properties are calculated by using average volume methods as represented by equation (12) and (13). Energy source term (the volumetric energy absorption rate) is represented by equation (14).

$$\left(\rho c_p\right)_{eff}\frac{\partial T}{\partial t} + \rho c_{pg}\left(u_g.\nabla T\right) = \nabla.\left(\lambda_{eff}\nabla T\right) + S_T \quad (11)$$

$$\lambda_{eff} = \varepsilon\lambda_g + (1-\varepsilon)\lambda_s \quad (12)$$

$$\left(\rho c_p\right)_{eff} = \varepsilon\left(\rho c_p\right)_g + (1-\varepsilon)\left(\rho c_p\right)_s \quad (13)$$

$$S_T = S_m(\Delta h) \quad (14)$$

$$\left(\rho_g c_{pg}\right)\left(\frac{\partial T}{\partial t} + u_g.\nabla T\right) = \nabla.\left(\lambda_g \nabla T\right) \quad (15)$$

$$\left(\rho_a c_{pa}\right)\left(\frac{\partial T}{\partial t} + u_a.\nabla T\right) = \nabla.\left(\lambda_a \nabla T\right) \quad (16)$$

Table 1: Metal hydride properties used in analysis (D'Entremont et al., 2018; Nyamsi and Tolj, 2021; Sheppard et al., 2014)

Properties	HTMH	LTMH
Reaction rate constant (1/s)	120000 (desorption)	175 (desorption)
Activation energy (kJ/mol)	102.5 (desorption)	52.2 (desorption)
Enthalpy of reaction (kJ/mol)	96.8	64.5
Entropy of reaction (J/mol K)	138	122.2
Specific heat capacity (kJ/kg K)	0.419	0.697
Gravimetric storage density (wt%)	2.5	3.6
Unsaturated density (kg/m^3)	1390	3200
Saturated density (kg/m^3)	1424.75	3315.2
Thermal conductivity (W/m K)	0.5	0.2

Assumptions

The assumptions considered in the numerical investigation are listed below.

- H_2 is assumed as an ideal gas.
- Thermal equilibrium between H_2 and MH are considered.
- The MH material is homogenous and isotropic.
- The effect of radiation inside the MH bed is not considered.
- The thermal properties of MH, H_2, and HTF are considered constant.
- The heat transfer between MH bed and surrounding is neglected.

Geometrical Parameters

The dimensions of the different domains of the dual metal hydride bed system considered in the numerical modeling are listed in Table 2. The diameter and height of the LTMH and HTMH bed, along with the dimensions of heat transfer fluid tubes and hydrogen supply tube, are listed below.

Table 2: Geometrical parameter of computational domain

Parameter	HTMH	LTMH
MH bed diameter (cm)	10.4	7.9
MH bed height (cm)	20.8	15.8
Diameter of H_2 tube (cm)	0.95	0.95
HTF tube inner diameter (cm)	0.44	0.44
HTF tube outer diameter (cm)	0.64	0.64
Number of HTF tubes	44	24

Initial Values

The initial values of different domains considered in the analysis are listed in Table 3 below.

Table 3: Initial values of different domains of HTMH and LTMH

Domain	$NaMgH_2F$ (HTMH)	Mg_2NiH_4 (LTMH)
Temperature of MH bed and HTF (ºC)	550	386.6
Pressure of MH bed (bar)	11.61	18.84
Temperature of H_2 (ºC)	25	25
Pressure of H_2 (bar)	1	1
Pressure of HTF (bar)	1	1
Density of MH bed (kg/m^3)	1390	3315.2

Thermodynamic cycle

The thermodynamic cycle of the MH bed for energy absorption and energy release process is shown in Figure 2. The energy release process takes place at point D where hydrogen movement is shown by dashed blue line from point A to D. The temperature of point D is 550ºC and due to the pressure difference between point A and D the movement of hydrogen takes place.

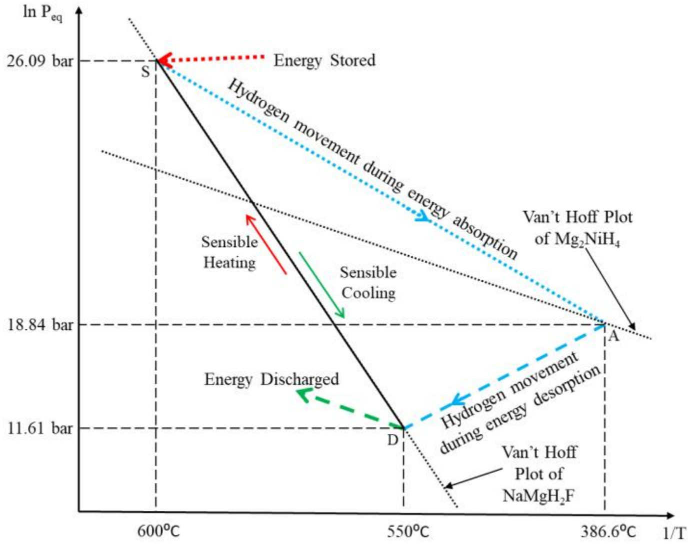

Figure 2: Thermodynamic cycle for dual MH bed TES system

Results and discussion

The study performed on the dual metal hydride bed system includes heat transfer analysis and energy desorption characteristics for variation of thermal conductivity of HTMH bed. Heat transfer analysis includes the study of temperature variation in the MH bed for different thermal conductivity of HTMH. The energy desorption characteristics include the evaluation of the quantity of energy released from the HTMH bed, the desorption rate, and the quantity of hydrogen absorbed in the HTMH bed.

During energy release from the HTMH bed, the average temperature of HTMH increases initially because of the exothermic reaction and the metal hydride bed releases more than 60% of thermal energy within 2000 seconds for all three cases of thermal conductivity. Figure 3 represents the variation of average metal hydride bed temperature with time for three different cases of thermal conductivity. With the increase in thermal conductivity of the MH bed, heat transfer from the MH bed is found to be improving and the MH bed temperature quickly attains the equilibrium temperature. The saturation fraction represents the fraction of thermal energy in the MH bed. The value of saturation fraction 1 means the MH bed is completely saturated with the thermal energy and no heat absorption will occur. The zero value of saturation fraction represents an empty MH bed. Figure 4 represents the saturation curve of the HTMH bed with time for different thermal conductivities. Due to effective heat transfer with higher thermal conductivity value, the metal hydride bed releases heat faster.

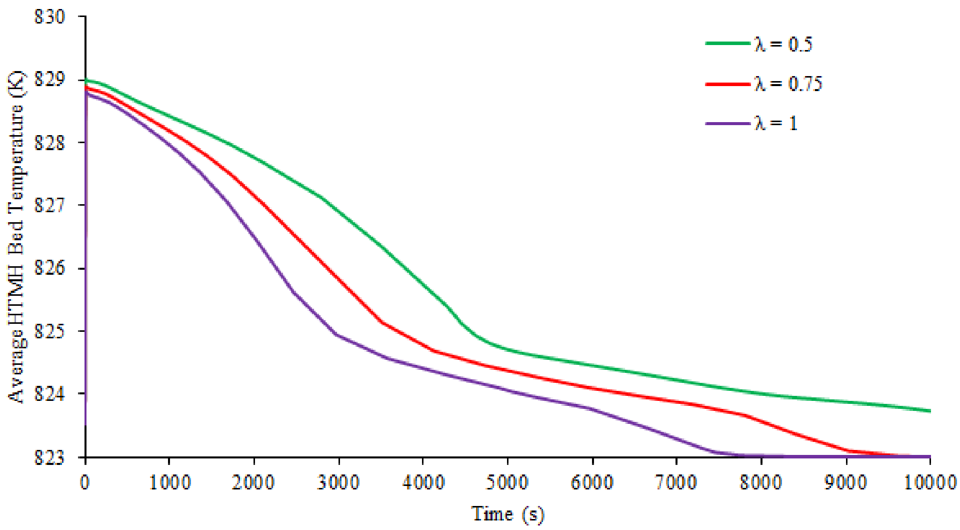

Figure 3: Average MH bed temperature variation of HTMH bed with time

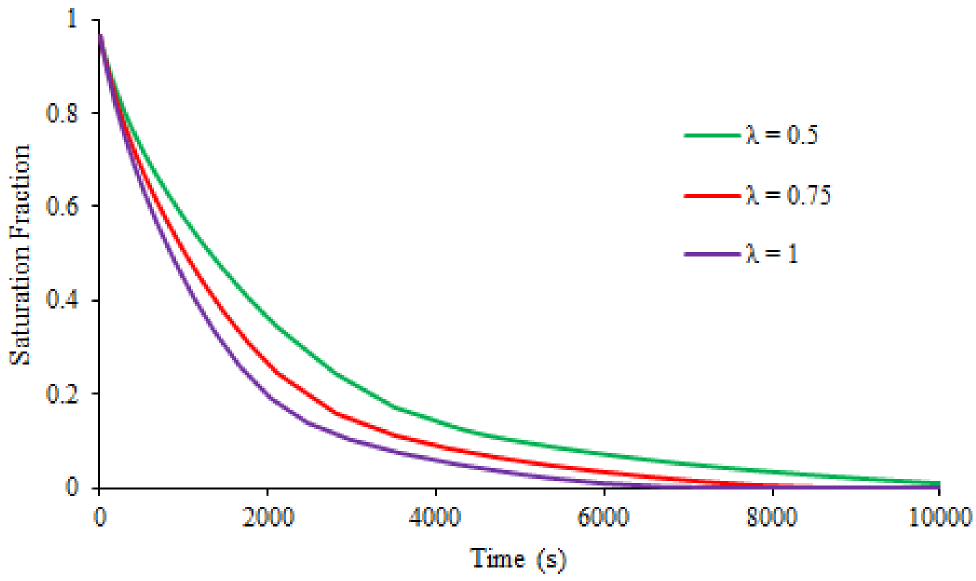

Figure 4: Saturation fraction variation of HTMH bed with time

Table 4 represents the saturation fraction value of the HTMH bed at different instants for three different thermal conductivity cases considered for analysis. The energy fraction available in HTMH bed at 500 s for 0.5 W/m K, 0.75 W/m K, and 1 W/m K thermal conductivity is found as 0.72, 0.67, and 0.64, respectively. Similarly, at 4000 s, the values are 0.14, 0.09, and 0.05, respectively. It shows that the energy release rate increases with the increase in thermal conductivity of the HTMH bed.

Table 4: Saturation fraction for different thermal conductivity at different instants during energy desorption

Time (s)	**Saturation Fraction (HTMH)**		
	0.5 (W/m K)	**0.75 (W/m K)**	**1.0 (W/m K)**
500	0.720686	0.677386	0.641221
1000	0.573917	0.502201	0.443264
2000	0.361458	0.264213	0.196231
3000	0.222463	0.145327	0.101345
4000	0.141797	0.090014	0.058569

The temperature contours and density contours for the energy release process at different instant is shown in Figure 5 and 6. The legend on the left in Figures 5 and 6 indicates the values for HTMH, while the right one indicates LTMH values. The cross-sectional temperature of HTMH is more uniform for high thermal conductivity. Due to improvement in heat transfer for higher thermal conductivity, the increase in temperature of HTMH bed is lesser and thus, the reaction kinetic is better in control rather than uncontrolled reaction due to higher temperature.

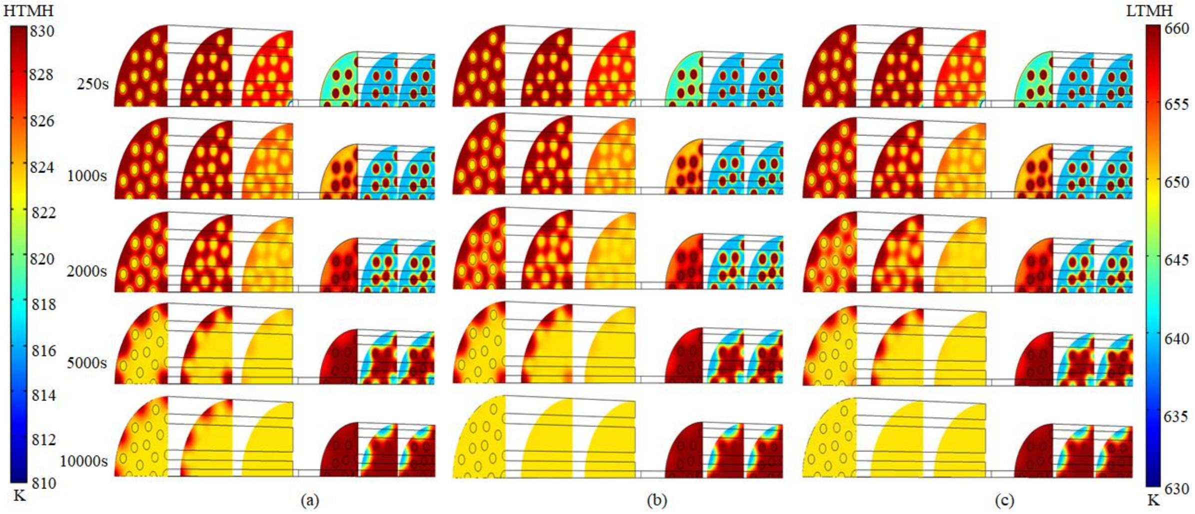

Figure 5: Temperature contours of dual MH bed for different thermal conductivity (a) 0.5, (b) 0.75, and (c) 1 W/m K

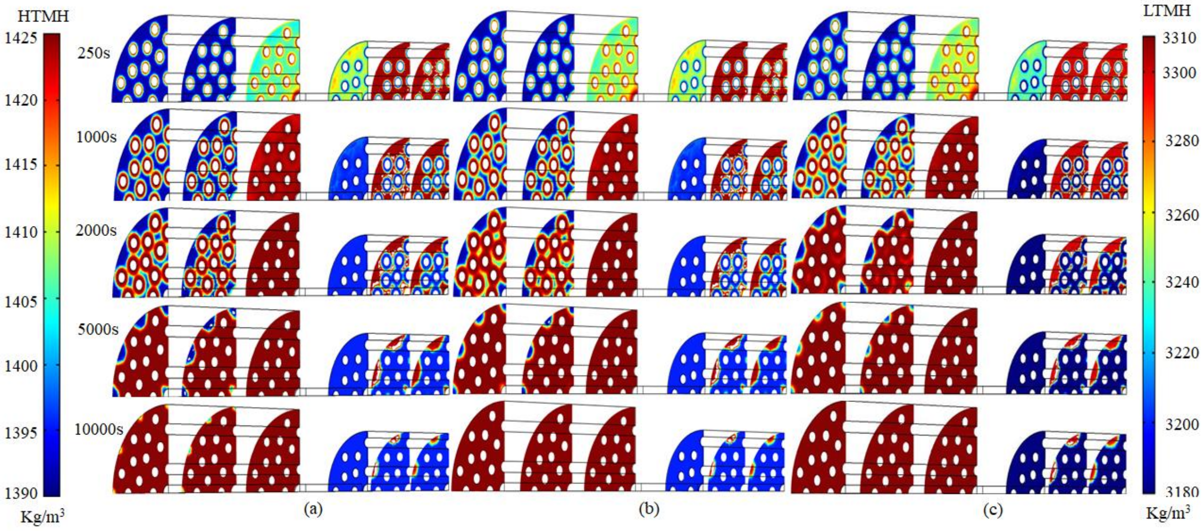

Figure 6: Density contours of dual MH bed for different thermal conductivity (a) 0.5, (b) 0.75, and (c) 1 W/m K

The energy released from the HTMH bed is found to increase with the thermal conductivity of the HTMH bed. The thermal energy release for 0.5 W/m K, 0.75 W/m K, and 1 W/m K thermal conductivity is found to be 251.25 kJ, 258.22 kJ, and 260.57 kJ, respectively. The quantity of hydrogen absorbed in the HTMH bed during energy release for 0.5 W/m K, 0.75 W/m K, and 1 W/m K thermal conductivity are found as 6.94 g, 7.13 g, and 7.17 g, respectively.

Conclusions

The heat transfer improvement due to an increase in the thermal conductivity of HTMH has shown better energy desorption characteristics. The key takeaways of the analysis are as follows:

- The increased thermal conductivity of the metal hydride bed leads to improved heat transfer rate from the HTMH bed.
- The release rate of energy has increased with the increase in the thermal conductivity of the HTMH bed.
- The energy release from the MH bed was found minimum for thermal conductivity 0.5 W/m K i.e., 251.25 kJ, and maximum for 1 W/m K i.e., 260.57 kJ.
- Hydrogen absorbed in the HTMH for thermal conductivity 0.5 W/m K, 0.75 W/m K, and 1 W/m K are 6.94 g, 7.13 g, and 7.17 g, respectively.

Acknowledgments

The authors are thankful to the Science and Engineering Research Board (SERB), Department of Science and Technology (DST), Government of India for awarding "Prime Minister Fellowship for Doctoral Research" to Mr. Sumeet Kumar Dubey in collaboration with Indian Oil Corporation Limited, Research and Development Centre and kind support from Confederation of Indian Industry (CII).

References

Bogdanović, B., Ritter, A., Spliethoff, B., Straßburger, K., 1995. A process steam generator based on the high temperature magnesium hydride/magnesium heat storage system. International Journal of Hydrogen Energy 20, 811–822. https://doi.org/10.1016/0360-3199(95)00012-3

D'Entremont., A., Corgnale, C., Sulic, M., Hardy, B., Zidan, R., Motyka, T., 2017. Modeling of a thermal energy storage system based on coupled metal hydrides (magnesium iron – sodium alanate) for concentrating solar power plants. International Journal of Hydrogen Energy 42, 22518–22529. https://doi.org/10.1016/j.ijhydene.2017.04.231

D'Entremont, A., Corgnale, C., Hardy, B., Zidan, R., 2018. Simulation of high temperature thermal energy storage system based on coupled metal hydrides for solar driven steam power plants. International Journal of Hydrogen Energy 43, 817–830. https://doi.org/10.1016/j.ijhydene.2017.11.100

Dubey, S.K., Kumar, K.R., 2022a. Charging and discharging analysis of thermal energy using magnesium nickel hydride based thermochemical energy storage system. Sustainable Energy Technologies and Assessments 52, 101994. https://doi.org/10.1016/j.seta.2022.101994

Dubey, S.K., Kumar, K.R., 2022b. Numerical investigation of energy desorption from magnesium nickel hydride based thermal energy storage system. Journal of Energy Systems 6, 165–175. https://doi.org/10.30521/jes.952627

Dubey, S.K., Kumar, K.R., 2021a. Numerical investigation of energy desorption from magnesium nickel hydride based thermal energy storage, in: 9th Eur. Conf. Ren. Energy Sys. Istanbul, Turkey, pp. 457–462.

Dubey, S.K., Kumar, K.R., 2021b. Numerical Investigation of Thermal Energy Storage using Magnesium Nickel Hydride, in: 26th National and 4th International ISHMT-ASTFE Heat and Mass Transfer Conference. pp. 577–583. https://doi.org/10.1615/IHMTC-2021.870

Jain, S., Dubey, S.K., Kumar, K.R., Rakshit, D., 2021. Thermal Energy Storage for Solar Energy, in: Fundamentals and Innovations in Solar Energy. pp. 167–215. https://doi.org/10.1007/978-981-33-6456-1_9

Malleswararao, K., N, A., Srinivasa Murthy, S., Dutta, P., 2020. Performance prediction of a coupled metal hydride based thermal energy storage system. International Journal of Hydrogen Energy 45, 16239–16253. https://doi.org/10.1016/j.ijhydene.2020.03.251

Nyamsi, S.N., Tolj, I., 2021. The impact of active and passive thermal management on the energy storage efficiency of metal hydride pairs based heat storage. Energies 14. https://doi.org/10.3390/en14113006

Paskevicius, M., Sheppard, D.A., Williamson, K., Buckley, C.E., 2015. Metal hydride thermal heat storage prototype for concentrating solar thermal power. Energy 88, 469–477. https://doi.org/10.1016/j.energy.2015.05.068

Sheppard, D.A., Corgnale, C., Hardy, B., Motyka, T., Zidan, R., Paskevicius, M., Buckley, C.E., 2014. Hydriding characteristics of NaMgH2F with preliminary technical and cost evaluation of magnesium-based metal hydride materials for concentrating solar power thermal storage. RSC Advances 4, 26552–26562. https://doi.org/10.1039/c4ra01682c

Sofiene Mellouli, Askri, F., Edacherian, A., Alqahtani, T., Algarni, S., Abdelmajid, J., Phelan, P., 2018. Performance analysis of a thermal energy storage based on paired metal hydrides for concentrating solar power plants. Applied Thermal Engineering 144, 1017–1029. https://doi.org/.1037//0033-2909.I26.1.78

Sunku Prasad, J., Muthukumar, P., 2023. Design of metal hydride reactor for medium temperature thermochemical energy storage applications. Thermal Science and Engineering Progress 37, 101570. https://doi.org/10.1016/j.tsep.2022.101570